Cluster State Quantum Computing

CIS:410/510 Final Report, Spring 2016

Dileep Reddy, Mayra Amezcua, Zach Schmidt
dileep@uoregon.edu, mamezcua@cas.uoregon.edu, zschmidt@cs.uoregon.edu

Abstract— **Any quantum computation can be performed via sequences of one-qubit measurements on a specific type of initially entangled state – the *cluster state*. Each computational step is a projective measurement that destroys a quantum state, leaving a final state that relies on the outcomes of earlier computations. The model of interest is the one-way quantum computer which is based on this measurement scheme. This paper will present background regarding computation using only measurements, a brief introduction into the preparation of cluster states, a discussion of one way quantum computers (1WQC), and the computational power of various configurations of a 1WQC.**

I. Background

Over the past few decades, advances in science and technology have greatly contributed to the development of modern computers. While these computers are efficient and convenient for everyday needs, they fail at certain computational tasks. Instead, quantum computers promise faster large scale factorization and database searches that are intractable for their classical counterparts. The first quantum computer designs were based off of classical models; sequences of one- and multi-qubit gate operations are performed on chosen quantum bits and a final measurement would convert quantum information into classical bits. A new model, proposed by Briegel and Raussendorf [1], demonstrates that quantum computation can be achieved by using single qubit measurements as computational steps. This so-called cluster model or *one-way quantum computer (1WQC)* relies on an entangled state of a large number of qubits or *cluster state* as the resource. The fascinating feature about 1WQC is that they have no classical analogues and probe into new territory in regards to entanglement and measurements.

II. Cluster States

Consider a set of qubits $\mathcal{C}$ labeled by an integer index, that are distributed in some lattice such that every qubit can be said to have adjacent neighbors. For these to collectively form a cluster state, their quantum mechanical state would be characterized by the set of eigenvalue equations [2],

$$K_a \left|\Phi\right\rangle_{\mathcal{C}} = \kappa \left|\Phi\right\rangle_{\mathcal{C}} \tag{1}$$

for a family of operators $K_a = X^{(a)} \bigotimes_{\gamma\in\Gamma(a)} Z^{(\gamma)}$, $a \in \mathcal{C}$, where $\Gamma(a)$ is the set of indices of all qubits in the "adjacent neighborhood" of a. The matrix $X^{(a)}$ is used to denote an X operation on qubit-a, and so on. The eigenvalue $\kappa = \pm 1$ is determined by the specific occupation pattern of the neighboring sites.

A. Preparation of linear cluster state

Intuitively, a cluster state can be thought of as a graph where every vertex represents a qubit, and every edge represents the application of a C_z gate to both adjacent vertices.

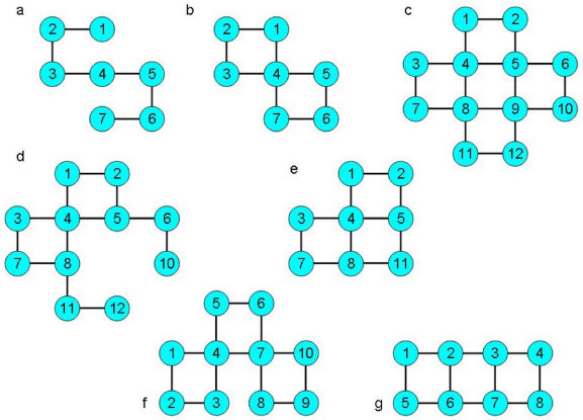

Fig. 1. Figure from [3], showing representative 2D cluster shapes. The vertices are qubits with integer indices, and the edges indicate entanglement connectivity between select neighbors.

A cluster state can be represented as a graph $G = (N, E)$, where the $n \in N$ is a qubit and $e \in E$ is the application of a Controlled-Z (C_z) gate, where:

$$C_z = \begin{pmatrix} 1 & 0 & 0 & 0 \\ 0 & 1 & 0 & 0 \\ 0 & 0 & 1 & 0 \\ 0 & 0 & 0 & -1 \end{pmatrix}$$

A *linear* cluster state is one where $degree(n) \leq 2 \forall n \in N$.

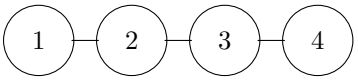

4-Node Linear Cluster State

A method to prepare such a cluster state is given in [4], consisting of "cascading" C_z gates on n qubits as follows:

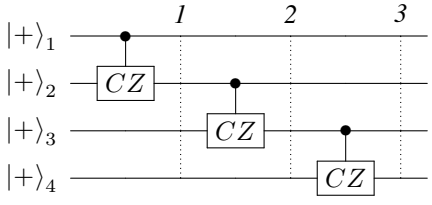

We can then analyze the state of the qubits at each of the dotted lines:

1:

$$\left(\frac{|0\rangle_1|+\rangle_2+|1\rangle_1|-\rangle_2}{\sqrt{2}}\right)|+\rangle_3|+\rangle_4$$
$$\equiv\left(\frac{|+\rangle_1|0\rangle_2+|-\rangle_1|1\rangle_2}{\sqrt{2}}\right)|+\rangle_3|+\rangle_4$$

2:

$$\left(\frac{|+\rangle_1|0\rangle_2|+\rangle_3+|-\rangle_1|1\rangle_2|-\rangle_3}{\sqrt{2}}\right)|+\rangle_4$$
$$\equiv\left(\frac{|0\rangle_1|+\rangle_2+|1\rangle_1|-\rangle_2}{2}|0\rangle_3+\frac{|0\rangle_1|-\rangle_2+|1\rangle_1|+\rangle_2}{2}|1\rangle_3\right)|+\rangle_4$$

3:

$$\left(\frac{|+\rangle_1|0\rangle_2|+\rangle_3+|-\rangle_1|1\rangle_2|-\rangle_3}{2}\right)|0\rangle_4$$
$$+\left(\frac{|+\rangle_1|0\rangle_2|-\rangle_3+|-\rangle_1|1\rangle_2|+\rangle_3}{2}\right)|1\rangle_4$$
$$\equiv\frac{(|+\rangle_1|0\rangle_2+|-\rangle_1|1\rangle_2)|0\rangle_3|+\rangle_4+(|+\rangle_1|0\rangle_2-|-\rangle_1|1\rangle_2)|1\rangle_3|-\rangle_4}{2}$$

The action of the C_z gate in the computational basis can be seen to be $|x,y\rangle \rightarrow (-1)^{xy}|x,y\rangle$. Cluster states of arbitrary shape and connectivity can similarly be prepared via the recursive use of the Hadamard gate and two-qubit fusion operations [5], [3].

B. Preparation of T-shaped cluster state

A cluster state without the limitation on the degree of a node allows us to build *nonlinear* cluster states:

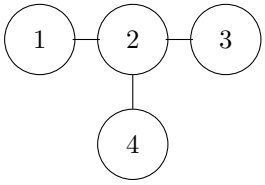

4-Node T-Shaped Cluster State

The circuit creating this cluster state will look as follows:

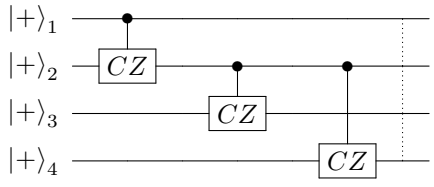

The state of the qubits after the application of the first two C_z gates is identical to the linear case, and the state after the last C_z (at the dotted line) is given by:

$$\frac{|+\rangle_1|0\rangle_2|+\rangle_3|+\rangle_4+|-\rangle_1|1\rangle_2|-\rangle_3|-\rangle_4}{\sqrt{2}}$$
$$\equiv\frac{1}{\sqrt{2}}\left[\left(\frac{|+\rangle_1|0\rangle_2|+\rangle_3+|-\rangle_1|1\rangle_2|-\rangle_3}{\sqrt{2}}\right)|0\rangle_4\right.$$
$$\left.+\left(\frac{|+\rangle_1|0\rangle_2|+\rangle_3-|-\rangle_1|1\rangle_2|-\rangle_3}{\sqrt{2}}\right)|1\rangle_4\right]$$

It is important to emphasize that the order in which the C_z gates are applied to grow the cluster state is irrelevant, as all of these pair-wise operations commute. This feature will be exploited later when discussing parallelizability.

III. The Effects of Measurement on a Cluster State

As is clear from the form of the expressions of all cluster states illustrated thus far, measuring any node in the computational basis severs it from the remaining graph by cutting all of it's edges with it's neighboring nodes. Should the outcome of said measurement be 1, then a Z gate/transform gets applied to all of it's erstwhile neighbors in the leftover cluster state. Thus, a large cluster state can be arbitrarily trimmed, split, and/or reshaped by removing qubits from the cluster. This is accomplished by measuring the target qubit in the computational basis, and performing appropriate unitary rotations on its former neighbors based on the measurement outcome.

The effect of an X-measurement (*i.e.,* a computational basis measurement following a Hadamard transformation) on any node of the cluster state is much more involved. This is best illustrated when demonstrating the use of a linear cluster state as a wire for quantum information. For this exercise, we start with a linear cluster state with three nodes (labelled 1, 2, and 3). A single qubit of quantum information $|\psi\rangle = \alpha|0\rangle + \beta|1\rangle$ is stored in a physical qubit labelled 0 as illustrated below.

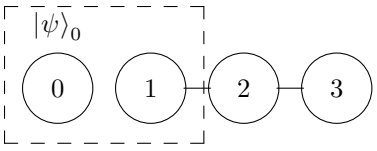

Gate $C_z^{(0,1)}$, followed by measurements $M_X^{(0)}$, $M_X^{(1)}$, & $M_X^{(2)}$.

To teleport the state $|\psi\rangle$ to physical qubit number 3, we must first supply the quantum information to the "wire." This is achieved by applying a C_z gate between physical qubits 0 and 1. Using $|\mathcal{LC}\rangle_{123}$ to denote the linear cluster state, we have

$$C_z^{(0,1)}|\psi\rangle_0\otimes|\mathcal{LC}\rangle_{123}$$
$$=\frac{1}{\sqrt{2}}[\alpha|0\rangle_0|+\rangle_1|0\rangle_2|+\rangle_3+\beta|1\rangle_0|-\rangle_1|0\rangle_2|+\rangle_3$$
$$\alpha|0\rangle_0|-\rangle_1|1\rangle_2|-\rangle_3+\beta|1\rangle_0|+\rangle_1|1\rangle_2|-\rangle_3]$$

Following this, we perform X-measurements on physical qubits 0, 1, and 2 in that order. Let us denote an X-measurement operation on the j^{th}-node with $M_X^{(j)}$, and let the outcome of any measurement on the same node be m_j. Then, the end result of these operations is the state

$$X^{m_2}Z^{m_1}X^{m_0}H|\psi\rangle_3, \qquad m_j\in\{0,1\}.$$

The quantum information $|\psi\rangle$ has successfully been teleported to physical qubit 3, up to application of Pauli operators depending on the measurement outcomes. Since the left-over/extra Pauli operators do not commute, these measurements had to have been carried out in a specific order. However, the operation $C_z^{(2,3)}$, which was employed to grow the linear cluster state, commutes with $C_z^{(0,1)}$, as well as measurements $M_X^{(0/1)}$. Thus, further links to the chain can be grown as earlier links are being subjected to measurements. This aids in parallelizability, as well as physical implementation of cluster state quantum computing schemes.

Briegel and Raussendorf show that any quantum logic circuit can be implemented on a cluster state, which demonstrates universality of the proposed scheme [1]. Nielsen [6] extended this result to no longer require coherent dynamics, instead relying on a method to teleport quantum gates, and he provided a concise algorithm to accomplish this.

IV. One-Way Quantum Computation

All quantum computation schemes may be characterized by some combination of state preparation, unitary transformation of said states, and measurements on the same. Human-usable computational tasks necessarily require both input and final output to be classical information. The classical input information can influence the quantum computation in choice of initial states, the choice of unitary transforms (*i.e.,* algorithm), and the choice of measurement bases. The output is always a classical function of the measurement outcomes. In typical models for quantum computation, entire algorithms are implemented as a sequence of unitary transformations on a prepared quantum state (stored in qubits) of size appropriate to the problem, with a round of measurements as the final step. In such models, the unitary transformation stage is completely reversible. The splitting of the effective unitary matrix into sequential steps can be arbitrary and entirely dependent on physical hardware limitations. There is no correspondence with "computational steps" or "clock cycles" in the classical sense, as the quantum state of the computer in the midst of the unitary stages is inaccessible for diagnosis or debugging purposes. Any leakage of information into computer memory or environment constitutes decoherence, and will introduce errors in the computation.

One-way quantum computation, on the other hand, revolves around single qubit measurements as a progression of computational steps. Measurements are a crucial component to quantum information processing because they irreversibly destroy a quantum state. Entanglement, on the other hand, will ensure that the state of the final qubit relies on the outcomes of preceding measurements. Given a cluster state, a series one-qubit measurements can be performed at each qubit to implement a quantum gate [4]. The unidirectionality of cluster state computation is inherent, due to the fact that quantum information cannot be accurately recovered once a measurement has been made. Consider a two-dimensional array of entangled qubits, information propagates horizontally through a row of qubits while vertical qubit neighbors are used for two-qubit gates. Similarly, three-dimensional clusters can be used to implement topologically protected gates [7], where the gate function only depends upon the way "connected defects" are wound around one another, but not on the details of their shape. This degree of freedom affords the design some fault tolerance.

The basic principle of cluster-state quantum computation is to effectively enact arbitrary quantum circuits onto qubits storing quantum information by performing single-qubit transformations and measurements on a pre-formed cluster state whose graph representation bears topological similarities to the circuit in question. These measurements result in destruction of the node-qubits of the cluster state, and hence are irreversible. The outcomes of these measurements need to be tracked or fed forward to influence future operations along certain layers of the cluster, as will be illustrated later in this article.

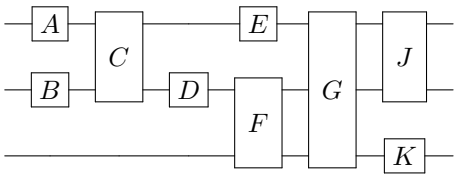

Arbitrary quantum circuit involving unitary operations on 3 qubits.

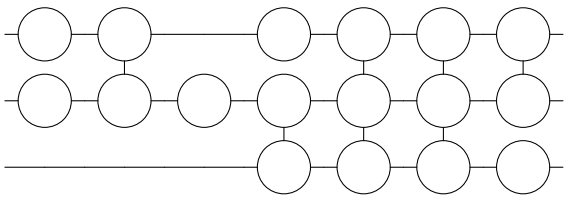

Single-qubit measurements on this cluster state is equivalent to the topologically similar circuit above.

A. Gates through teleportation

Quantum teleportation is a procedure by which quantum information can be transferred from one point to another via two classical bits of information if the sender and received previously shared an entangled state. It is useful for quantum computation however, this approach uses an entangled state as a resource but if that state has some error then teleportation fails. Gottesman and Chuang [8] first showed that if the entangled state $|\psi\rangle$ can be replaced by $U|\psi\rangle$, such that U is a non-trivial quantum operation. The corresponding output $U|\alpha\rangle$ is in the initial state $|\psi\rangle$ but with additional single-qubit Pauli operations X, Y, or Z. By simply reversing the Pauli operators the original state can be reconstructed. This teleportation scheme can be useful in applying other gates that are non-trivial.

$$HZ_\alpha = \frac{1}{\sqrt{2}} \begin{pmatrix} e^{\frac{-i\alpha}{2}} & e^{\frac{i\alpha}{2}} \\ e^{\frac{-i\alpha}{2}} & -e^{\frac{i\alpha}{2}} \end{pmatrix}$$

As demonstrated in the previous section, by applying single-qubit gates we can teleport one state from one side of a cluster state to the other. In this section we demonstrate how to apply the HZ_α gate through teleportation.

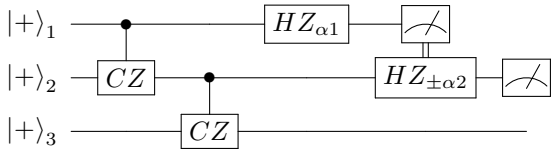

In this example we will apply two consecutive HZ_α gates to our cluster to simulate two gates on a single qubit. We will demonstrate that the outcome is the same except for an additional two Pauli operations. For this problem we prepare a three node cluster state given by:

$$C_z^{(1,2)} C_z^{(2,3)} |+\rangle_1 |+\rangle_2 |+\rangle_3 = |\psi_1\rangle$$
$$= \frac{1}{\sqrt{2}} |0\rangle_1 (|0\rangle_2 |+\rangle_3 + |1\rangle_2 |-\rangle_3)$$
$$+ \frac{1}{\sqrt{2}} |1\rangle_1 (|0\rangle_2 |+\rangle_3 - |1\rangle_2 |-\rangle_3)$$

First we will apply $HZ_{\alpha 1}$ and measure in the computational basis.

$$HZ_{\alpha 1} |\psi_1\rangle = \frac{e^{-i\alpha_1/2}}{2} |+\rangle_1 \left(\frac{|0\rangle_2 |+\rangle_3 + |1\rangle_2 |-\rangle_3}{\sqrt{2}} \right)$$
$$+ \frac{e^{i\alpha_1/2}}{2} |-\rangle_1 \left(\frac{|0\rangle_2 |+\rangle_3 - |1\rangle_2 |-\rangle_3}{\sqrt{2}} \right) = |\psi_2\rangle$$

For convenience we assume that we measure the state $|0\rangle$.

$$X^0 |\psi_2\rangle = \frac{1}{\sqrt{2}} \cos(\alpha_1/2) |0\rangle_2 |+\rangle_3$$
$$- \frac{i}{\sqrt{2}} \sin(\alpha_1/2) |1\rangle_2 |3\rangle_3 = |\psi_3\rangle$$

We apply one final HZ_α gate.

$$HZ_{\pm\alpha 2} |\psi_3\rangle = |\psi_4\rangle$$
$$\frac{1}{\sqrt{2}} |0\rangle_2 \left(\cos(\frac{\alpha_1}{2}) e^{-i\alpha_2/2} |+\rangle_3 - i \sin(\frac{\alpha_1}{2}) e^{i\alpha_2/2} |-\rangle_3 \right)$$
$$+ \frac{1}{\sqrt{2}} |1\rangle_2 \left(\cos(\frac{\alpha_1}{2}) e^{-i\alpha_2/2} |+\rangle_3 + i \sin(\frac{\alpha_1}{2}) e^{i\alpha_2/2} |-\rangle_3 \right)$$

The final output state we get is:

$$X^0 |\psi_4\rangle = |\psi_5\rangle = \frac{1}{\sqrt{2}} \cos(\frac{\alpha_1}{2}) e^{-i\alpha_2/2} |+\rangle_3$$
$$- \frac{i}{\sqrt{2}} \sin(\frac{\alpha_1}{2}) e^{i\alpha_2/2} |-\rangle_3$$

The output of the circuit is $X^{m_2} HZ_{\pm\alpha 2} X^{m_1} HZ_{\alpha 1} |+\rangle_3$, where m_1 and m_2 are the outputs for the first and second qubits. Analyzing this output a bit further we see that $HX^{m_1} = Z^{m_1} H$ and $Z_{\pm\alpha 2} X^{m_1} = X^{m1} Z_{\alpha 2}$. Using this the state can be rewritten as:

$$X^{m_2} Z^{m_1} HZ_{\alpha 2} HZ_{\alpha 1} |+\rangle_3$$

This is equivalent to the output of the conventional single-qubit quantum circuit up to a known Pauli matrix. Thus it is easy to model gate application through teleportation.

We observe that in the circuit given below the two highlighted boxes are both one-bit teleportations. Because the C_z gate commutes with HZ_α we can perform one teleportation procedure and then the second one or vice-versa. This is advantageous because it means that we can build the cluster as we go.

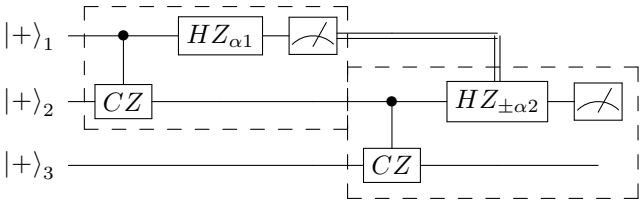

B. Applying a 2-qubit gate via 2D cluster state

The ability to implement gates of the form HZ_α, and any 2-qubit controlled-phase gate, and to prepare arrays of $|+\rangle$ states as inputs, constitute a set of resources that is universal for quantum computation [9]. In this subsection, we will demonstrate the use of two-dimensional cluster states to implement a C_z gate between two input kets bearing quantum information $|\phi_A\rangle_A |\phi_B\rangle_B$ encoded in physical qubits labelled 'A' and 'B.' Here, $|\phi_j\rangle := \alpha_j |0\rangle + \beta_j |1\rangle$. For the scheme, we will use an I-shaped cluster states with six nodes, as shown in the figure.

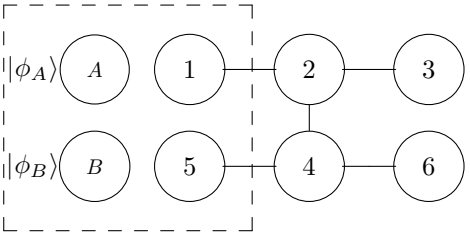

Apply $C_z^{(A,1)}$ and $C_z^{(B,5)}$ to input quantum information into cluster state.

The procedure would be to first entangle the input quantum information qubits into the cluster state via the application of C_z gates. Then we perform single qubit measurements on all qubits but numbers 3 and 6. Using the Z-measurement property of nodes on cluster states, we can pick node 4 as a representative anchor and write down the total state of the current system as

$$\frac{1}{\sqrt{2}}\left[\left|\mathcal{LC}\right\rangle_{123}\left|0\right\rangle_4\left|+\right\rangle_5\left|+\right\rangle_6 + Z_2\left|\mathcal{LC}\right\rangle_{123}\left|0\right\rangle_4\left|-\right\rangle_5\left|-\right\rangle_6\right] \otimes \left|\phi_A\right\rangle_A\left|\phi_B\right\rangle_B ,$$

where Z_2 is being applied on qubit 2.

The single qubit mesurements have to be performed in the order $(M_X^{(A)}, M_X^{(1)}, M_X^{(2)})$ and $(M_X^{(B)}, M_B^{(5)}, M_X^{(4)})$. These two subsets are parallelizable, and one could perform the measurements $\{M_X^{(A)}, M_X^{(B)}\}$ in parallel, and then $\{M_X^{(1)}, M_X^{(5)}\}$, and so on. But here, we will introduce the concept of layers of measurement, by performing all bottom row operations at once (including input entanglement), and then working on the top row.

Enacting the gate $C_z^{(B,5)}$ on the initial state, followed by measurements $M_X^{(B)}, M_B^{(5)}, M_X^{(4)}$ yields random outcomes $m_B, m_5, m_4 \in \{0,1\}$ and gives us the state

$$X_6^{m_4} Z_6^{m_5} X_6^{m_B} C_Z^{(2,6)} \left|\mathcal{LC}\right\rangle_{123}\left|\phi_B\right\rangle_6 \otimes \left|\phi_A\right\rangle_A .$$

Note that even though the original cluster state had an edge between nodes 2 and 4 in the graph representation, a measurement on qubit 4 did not sever the link between node 6 and the linear chain $\left|\mathcal{LC}\right\rangle_{123}$, due to the measurements being in the X basis. Now, if we follow the above operations by application of the $C_Z^{(A,1)}$ gate, and the measurements $M_X^{(A)}, M_X^{(1)}, M_X^{(2)}$ in that order, we get the random results $m_A, m_1, m_2 \in \{0,1\}$ and the final state

$$X_3^{m_2} Z_3^{m_1} X_3^{m_A} H_3 X_6^{m_4} Z_6^{m_5} X_6^{m_B} H_6 C_X^{(6,3)} \left|\phi_A\right\rangle_3\left|\phi_B\right\rangle_6 ,$$

where $C_X^{(j,k)}$ is the controlled-NOT gate. All single-qubit operations on qubit 3 commute with single-qubit operations on qubit 6. Using the fact that $H_j^2 = I_j$, as well as $C_X^{(6,3)} \equiv (H_3 \otimes I_6) C_Z^{(3,6)} (H_3 \otimes I_6)$, the final state is equivalently

$$X_3^{m_2} X_6^{m_4} Z_3^{m_1} Z_6^{m_5} X_3^{m_A} X_6^{m_4} H_6 C_Z^{(3,6)} H_3 \left|\phi_A\right\rangle_3\left|\phi_B\right\rangle_6 ,$$

which is the desired result, up to overall Pauli transformations on the individual qubits. Thus, we have proven that a universal set of quantum operations can be implemented using the cluster state model.

C. *Commutations and parallelizability*

The previous subsections demostrated that although measurements in a specific layer (an ordered set of sequentially connected nodes) of a cluster state need to occur in a specific order, operations on different layers commute, and can therefore be interspersed. This, combined with the ability to delay the growth of the cluster state to occur just before the measurements catch up with the remaining nodes, offers several possibilities for process parallelization.

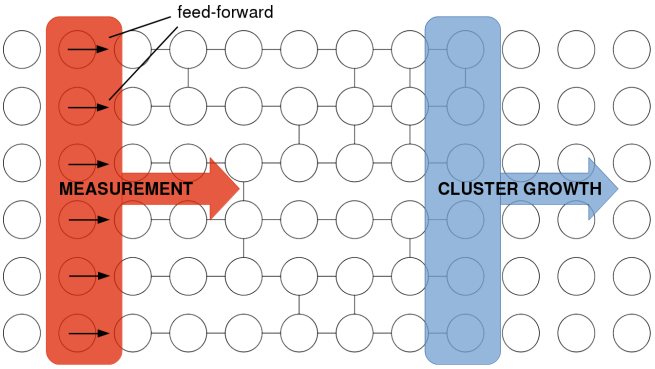

Fig. 2. The controlled-phase operations commute with unitaries and measurements on other parts of the cluster state. This allows one to conserve and reuse physical resourses, as well as maintain coherence on smaller cluster sizes at any given time.

Indeed, in the 2-qubit gate example, the quantum information in one of the qubits was put into the system first, followed by some measurement-based teleporation, and the other input qubit was brought in later. We effectively managed to entangle the two qubits using only single-qubit measurements.

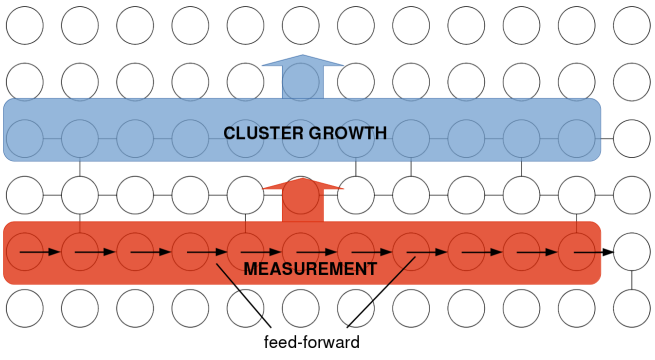

Fig. 3. X-measurements do not sever "vertical" links despite destruction of qubits. This allows different linear layers to be processed in any order.

This seems to indicate that all multi-qubit interactions can be pre-computed by setting the topological layout of the graph of the cluster state before any of the quantum information has even been introduced into the system.

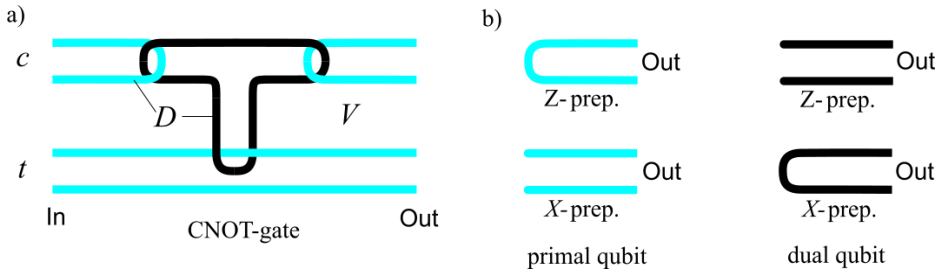

Fig. 4. Figure from [10]. Topologically protected gates as realized in three-dimensional cluster states. (a) An individual encoded CNOT gate with control c and target t. (b) The preparation of logical qubits in the $\{|0\rangle, |1\rangle\}$ (*i.e., Z*-) and the $\{|\pm\rangle\}$ (*i.e., X*-) bases. The line-like structures are connected defect sites (nodes measured in the Z-basis, denoted by set 'D') embedded in a 3D lattice, surrounded by sites belonging to set 'V' (measured in the X-basis). The gate function only depends upon the way the defect lines are wound around one another.

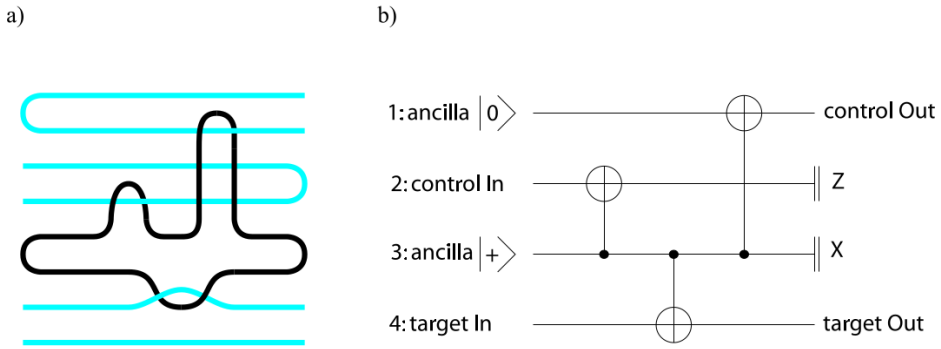

Fig. 5. Figure from [10]. (a) Another version of the CNOT gate topologically equivalent to that shown in figure 4(a). (b) Equivalent circuit, representing a CNOT gate between the control and target qubit.

D. 3D cluster states and topological fault tolerance

While 2D cluster states are sufficient for fully realizing any quantum computation, Goyal et al [10] have exploited a correspondence between quantum gates, quantum correlations, and surfaces to propose a topological model for cluster-state quantum computation. The method affords them a (fault-tolerance) threshold estimate of 0.75% for each source in an error model with preparation, gate, storage and measurement errors, with a poly-logarithmic multiplicative overhead in the circuit size. While a full detailed description of this approach is beyond the scope of this article, here we present a brief overview.

In their scheme, a 3D cluster state consisting of a lattice of qubits is 'carved out' with 1D line-like defects via Z-measurements on connected physical qubits. This results in a nontrivial cluster topology in which a fault-tolerant quantum circuit is embedded (figure 4). These line defects essentially simulate anyons [11], and the way they knot and loop around each other effectively obeys non-Abelian braiding statistics, allowing one to simulate gates (figure 5). The fault tolerance comes from the topological invariance of the structures to local perturbations to the line defects (such as specific path and length). One of the dimensions of this 3D representation can be mapped to 'simulated time,' which is a necessary facet of all computation that maps inputs to outputs. This mapping can be literal in physical 2D cluster states.

V. Computational Power and Complexity

The spacial layout of the graph representation of the cluster state plays a role in the computational power of that state. If a cluster state can be prepared linearly via the cascading C_z technique mentioned above, it can be represented as a "one-dimensional" graph (i.e., some graph $G = (V, E)$, $\forall v \in V$, $\deg(v) \leq 2$). Operations on a linearly prepared cluster state can be efficiently simulated on a classical computer in $O(n \log^c(1/n))$, where n is the initial number of qubits, and c is the cost of floating point multiplication [12]. Though the author consequently dismisses linearly prepared cluster states as a substrate for quantum computation, it would be interesting to know which class of problems they would be able to solve.

A. Gate array reductions

With only a bit of construction, it can be seen that the cluster state model is polynomially reducible to the gate array model, and the converse is also true. To see this, we first need to create a definition of the standard gate array model:

1. All measurements take place at the end of the circuit
2. All measurements take place in the computational basis

We can now generalize this definition to allow measurements along the way with subsequent choices of gates and measurements being allowed to depend on earlier measure-

ment outcomes. Intuitively, what we will do is add an ancilla bit to all measurements which take place before the end, and perform controlled operations with this ancilla to return to the standard definition. Specifically, for all measurements in the $\{U|0\rangle, U|1\rangle\}$ basis, we add an ancillary qubit A, (initially in state $|0\rangle$) and replace the measurement with an application of $U^\dagger$ to B followed by applying C_X to BA as shown:

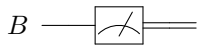

Fig. 6. Some non-standard circuit

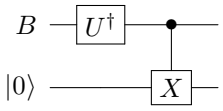

Fig. 7. An equivalent standard circuit

Now, any future gates that depended on the measurement outcome are replaced by a corresponding controlled operation, controlled by the state of A. It is therefore clear that this process converts any non-standard circuit to the standard gate array model.

A.1 Reducing cluster state to gate array

The above technique shows how a cluster state circuit is converted into an equivalent (standard) gate array. In addition to building the required cluster state using an array of C_Z gates acting on $|+\rangle$ states, we introduce an ancilla A for each 1-qubit measurement. For each $M(\theta)$ measurement we introduce an extra gate $W^\dagger(\theta)$ which transforms the $M(\theta)$ basis to the standard basis.

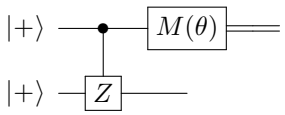

Fig. 8. A two qubit cluster state

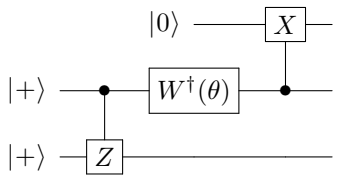

Fig. 9. An equivalent cluster state with ancilla

Thus, to convert the measurement-based cluster state model to the gate array model requires polynomially more gates and qubits (one per measurement).

A.2 Reducing gate array to cluster state

To see how an arbitrary gate array can be converted to the cluster state model, we first need some universal gate set G (for information on what this set might contain, see [13]). For each gate within this set, we can specify some number which represents the number of measurements that a 1WQC would have to perform to get the same outcome. These numbers can then be used to partially order a set, allowing us to pick K, which represents the maximum number of measurements required to simulate any single gate from the set. From this, we can see that even if some circuit contained only this "most expensive" gate, the number of additional qubits and gates would be a factor of K (polynomial).

B. Quantum layers

The above reduction strategy provides a nice way of categorizing a given quantum algorithm into its classical and quantum parts:

- The classical parts are those that are done serially (i.e. the decision of future gates based on measurement outcomes)
- The quantum parts are those that can be done in parallel

From this, we can see that the cluster state model exemplifies both parts, but the gate array model only does "quantum parts". With this idea, we can define the notion of layers by saying that a quantum process with K layers is one where K gates are operating in parallel. The above suggests the following conjecture [9]:

Conjecture: Any polynomial time quantum algorithm can be implemented with only $O(\log n)$ quantum layers interspersed with polynomial time classical computations.

This conjecture remains unproven in general, but it has been shown to hold for Shor's algorithm [14].

C. Cluster graphs as an analysis tool

Outside of the physical implementation considerations, cluster state model isomorphisms offer a new analysis tool that disentangles the quintessential influence of quantum formalism on the complexity class of various algorithms.

We have already shown in section IV, how any quantum algorithm that is expressible via a quantum gate-array circuit can equivalently be computed via single-qubit operations and measurements on a cluster state represented by a graph whose connectivity is topologically similar to the circuit diagram. This equivalence is purely geometric and is independent of the specific gates being applied (those are determined by the choice of measurements on the cluster state). This allows us to reduce entire classes of algorithms to specific types of graphs with designated input and output nodes for state-preparation and final-result measurements. We conjecture that the size of this graph has a bearing on the computational time of the entire class of algorithms. Furthermore, the multi-dimensional connectivity of said graphs embodies entangling operations, and serves to explicitly quantify any gains in complexity quantum offers over classical methods. And finally,

the connectivity and feed-forward paths allows one to define modular operations that are independent of each other, and can help exploit all avenues for parallelization more effectively.

VI. Physical implementations

Although the chief inspiration for cluster-state quantum computation was the ability to enact gates via teleportation, another motivation proved to be the extant experimental realizations of material qubits arranged in 2D arrays in physical space; be they cold atoms in optical lattices [15], or 2D ion traps [16], or other stationary qubits embedded in material substrates (quantum dots, superconducting qubits). The geometry of such systems encourages designs involving programming a quantum circuit into the device by literally "etching" the circuit diagram onto the 2D qubit array.

Given the prevalence of experiments on 2D lattices of physical qubits, it is natural to ask if it were possible to anneal such a system in an imposed, time-invariante potential such that the natural ground state of the corresponding Hamiltonian would be a desired cluster state. Nielsen [12] provides an argument for why this is not possible for systems that have only two-body interactions (up to first order). The "distance" between any cluster state and the energy eigenstates of a Hamiltonian with two-body interactions of the connection-intended qubit pairs can be shown to be bounded below by a constant independent of anything except the Hilbert space dimension (*i.e.,* the cluster size).

A. Two qubit operations on non-photonic matter qubits

The above argument however, does not forbid the application of time-varying interaction potentials in order to facilitate inter-qubit entangling operations. In matter qubits that have physical proximity, this can be achieved by applying external electric and magnetic fields. For example, two neighboring quantum dots with one valence electron each, can be coupled via transverse electric and magnetic fields to implement a quantum XOR gate via an exchange mechanism [17]. Figure 10 illustrates the essential mechanism. The coupling fields are pulsed such that the net integral effect of the interaction results in a "swap" operator being applied. The temporal duration of the unitary time-evolution operator associated with the interaction naturally depends on the physical parameters in question, namely, the quantum dot size, mutual distance between them, peak field strength, etc.

For trapped ions and neutral atoms, two-qubit gates can be enacted by coupling internal degrees of freedom in individual qubits (usually electron energy levels) with multi-qubit vibrational modes. For ions [18], the interaction is mediated by the Coulomb potential, whereas in neutral atoms [19], this could be due to dipole-dipole interactions between atoms excited to low-lying Rydberg states in constant electric fields. The state read-in, single-qubit manipulation, and state read-out are all carried out using coherent laser pulses of set power and durations. The durations are dictated by the natural Hamiltonian frequencies of the energy states being coupled, and the pulses are designated names such as π-pulses in the literature, depending on their effect in the Hilbert space.

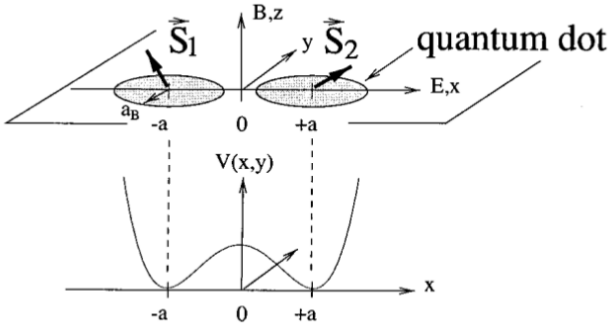

Fig. 10. Figure from [17]. Two coupled quantum dots with one valence electron per dot (both confined to the xy plane). Their spins are denoted by $\vec{S}_1$ and $\vec{S}_2$. The magnetic field B is along the z-axis and the electric field E is along the x-axis. The interaction term of the Hamiltonian reads $H_s(t) = J(t)\vec{S}_1 \cdot \vec{S}_2$, where the exchange coupling j between the spins is a function of B, E, and the interdot distance $2a$.

A common feature of all such physical systems is the profusion of degrees of freedom available for manipulation. The storage of quantum information typically occurs within well chosen, two-level subspaces of the full Hibert space, which are local (non-interacting) and relatively decoherence free. All multi-qubit operations, however, occur in higher-energy, nonlocal regions of the Hilbert space. The storage subspaces and the interaction subspaces are temporarily coupled to each other via externally applied potentials for the necessary duration for specific types of interactions to occur.

B. Nondeterministic two-qubit gates with linear optics

Matter qubits are promising candidates for quantum computing but they are subject to decoherence. Photons, on the other hand, do no suffer from decoherence effects because they weakly interact with the matter. However, multi-qubit operations on photons are much harder because of this weak interaction. A new approach fuses photon states into entangled states via projective measurements. With this method, nondeterministic multi-qubit gates can be applied to photons. KLM [20] showed that this method can be used for efficient quantum computation using linear optical elements only. It can be carried over to preparation of cluster states.

The second section of this paper discussed how to construct a T-shaped cluster state by entangling qubits 2 and 4. A linear cluster state can be grown on qubit 4 to create a 2D cluster state. However, this method cannot be easily applied to photons with high fidelity. Browne and Rudolph [5] first proposed a scheme to build L-shaped clusters using two different fusion types. The L-shaped structures would provide an easy way to construct 2D arrays. In 2006, Gilbert et. al. [3] proposed a simpler scheme which used local unitaries and type-I

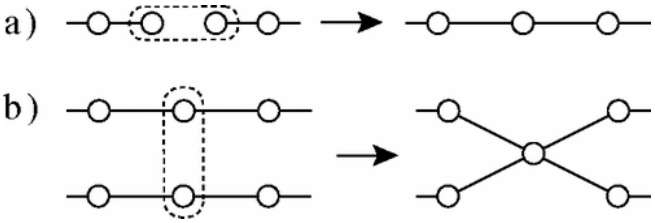

Fig. 11. Figure from [5]. (a) Connceting the end qubits of two linear cluster states using type-I fusion. (b) Middle qubits are fused to create a cross in the cluster state.

fusion operations to create a two-dimensional cluster state. By only utilizing type-I fusion Gilbert et. al. demonstrated that the cost of creating an entangled state was reduced from 34 bonds to 2 bonds. Type-I fusion takes the end qubits of two separate linear clusters and makes a projective measurement. The fusion of the two linear clusters would be determined by the number of photons that were measured. If one photon was measured the two clusters would be joined with $(n+m-1)$ qubits, or the two clusters would remain separate. If the fusion operation were to fail, the size of each cluster would be reduced by one qubit (or split, if fusion was attempted in the middle), and the fusion will have to be reattempted.

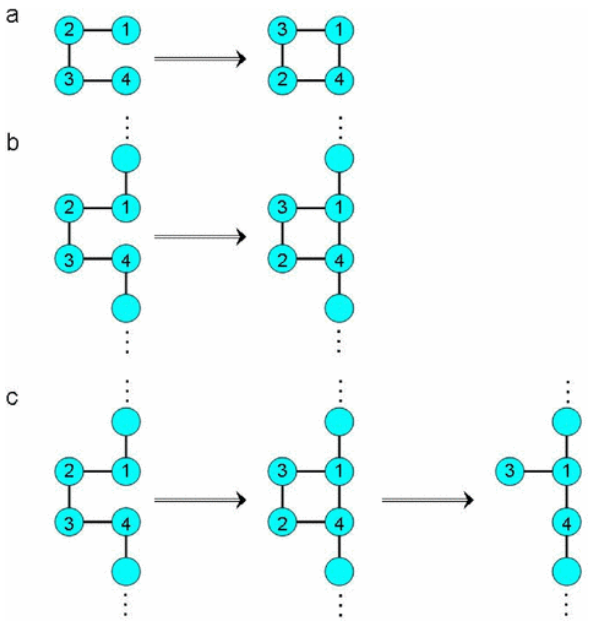

Fig. 12. Figure from [3]. (a) Hamdamard gate applied to qubits 2 and 3. (b) The operations prepare this box state which entangles qubits 1 and 4. (c) Once the box is formed a measurement is made on qubit 2 to break the bonds and create the L-shaped structure.

The first photonic cluster state was created by Zhang et. al. in 2005 [21]. This three qubit linear cluster was created by generating pairs of entangled photons and using Type-I fusion between photons in paths 2 and 3. The final entangled state was measured using photodetectors and verified with the three particle Bell inequality.

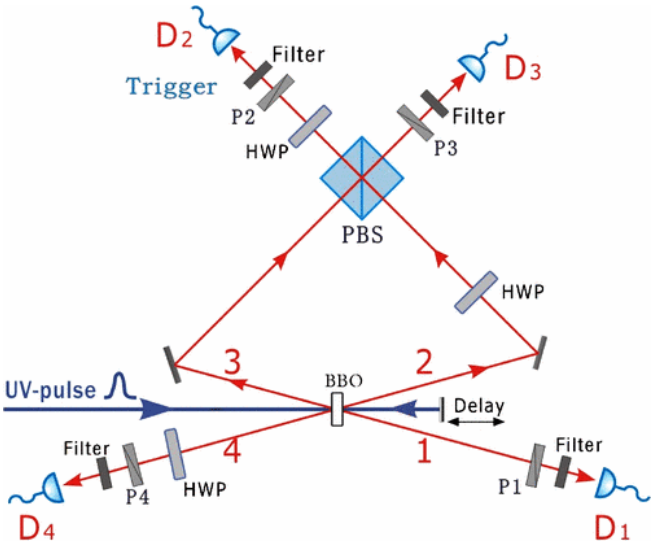

Fig. 13. Figure from [21]. Two pairs of entangled photons are created via spontaneous parametric down conversion. Opposite pairs are sent through polarizing beam splitters to do type-I fusion and then detected to verify the state.

C. Continuous-variable cluster states

While single-photons have sufficent degrees of freedom to afford storage of quantum information, the difficultly of causing multiple photons to efficiently interact with each other limits their potential. However, the interaction barrier can be circumvented by relying on cavities, and the quadrature space of optical modes for information storage. Squeezed coherent states of light [22] are specific linear combinations of photon-number states in a designated set of optical modes. In quadrature space, they are expressed as Gaussian functions with well defined axes of squeezing. The widths of the major and minor axes refer to the quantum uncertainty in two canonical (non-commuting) quadrature expectation values. The uncertainties are saturated to the Heisenberg limit, but the asymmetry results in one quadrature uncertainty having been drastically reduced at the expense of the other.

Quadratures make for a perfectly acceptable Hilbert space of infinite dimension. They can be entangled, and by extension, can be used as a quantum resource to teleport other continuous variable states. Multiple optical modes are generally squeezed via a process of spontaneous parametric down conversion (SPDC), where in a coherent laser pump field of a higher frequency interacts with a bulk, nonlinear material (typically a down-conversion $\chi^{(2)}$ crystal or crystalline waveguide) to produce pairs of correlated photons at a lower frequency. If this process were to occur inside an optical cavity whose modes are resonant at the emitted field frequencies, then the interaction is no longer perturbative, and will result in significant squeezing. Such sources are called optical parametric oscillators (OPO).

Multiple optical modes (defined by beam-momentum vec-

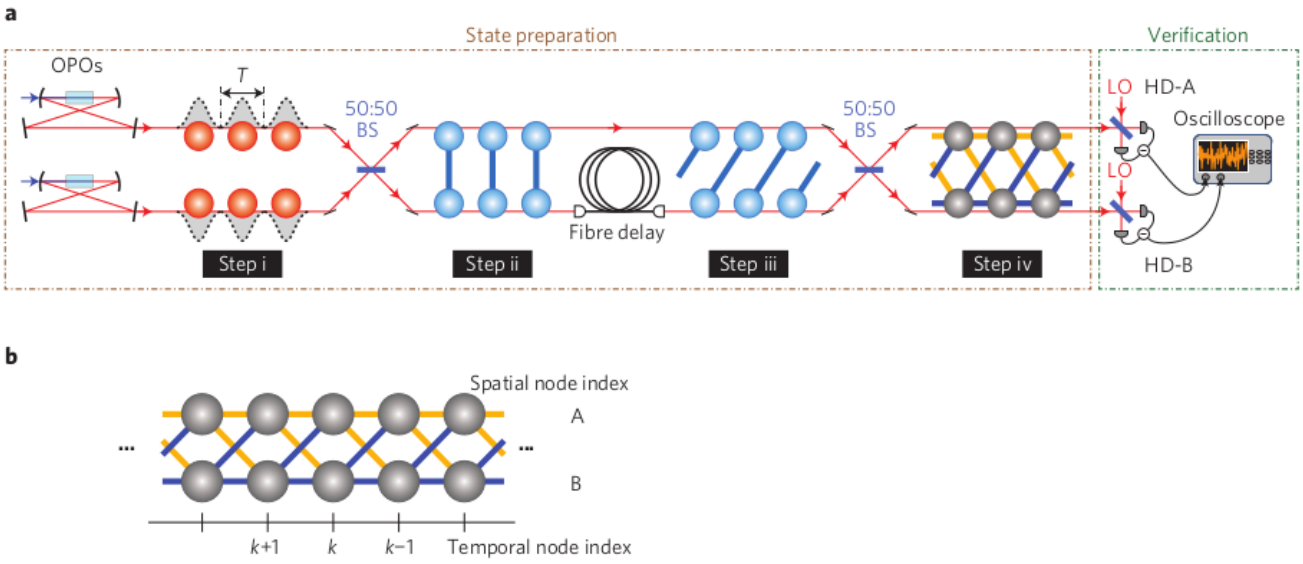

Fig. 14. Figure from [23]. Yokoyama et al use (a) two separate optical parametric oscillators (OPOs) as sources of squeezed pulses of light, and mix them in an unbalanced Mach-Zehnder interferometer to produce (b) a long, dual-rail style squeezed state. 50:50 BS, balanced beamsplitter; HD, homodyne detector; LO, local oscillator.

tors) may then be deterministically entangled in quadrature space via use of linear optical elements such as simple beam splitters. Yokoyama et al [23] exploited this to create a lengthy continuous variable cluster state encoded in quadratue space (figure 14). An optical cavity has multiple resonant modes at different frequencies, and a sufficiently broadband SPDC process can squeeze many of them in pairs. By using two pumps at different polarizations and slightly offset frequencies, Chen et al [24] managed to generate the same lengthy cluster state, with the time-multiplexed axis having been replaced by a discrete frequency variable in some spiral magnitude order (figute 15).

Continuous variable cluster states cannot be used for quantum computation if all our manipulation and measurement operations are so-called "Gaussian" in nature. For optical quadrature squeezed cluster states, measurement in the photon-number basis is a non-Gaussian operation, and might be sufficient to break the constraint. Such optical cluster states, however, are by definition travelling at the speed of light, and barring a sophisticated quantum memory solution, will require computational steps to occur on the fly using ultrafast homodyne detection setups.

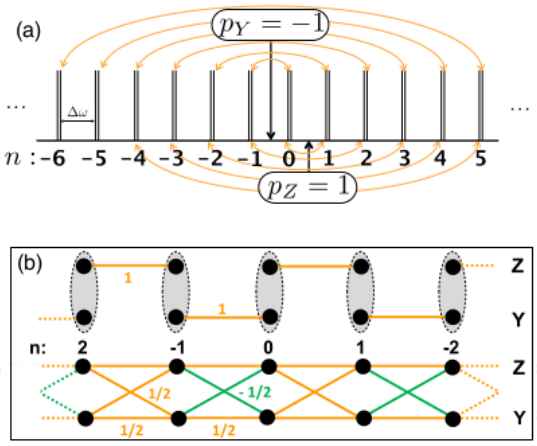

Fig. 15. Figure from [24]. Chen et al pumped an OPO with two pumps with perpendicular polarizations (Z and Y) and offset frequencies to couple th squeezing of intertwined pairs of (a) optical cavity-resonant modes. These are then mixed on a single beamsplitter to produce (b) a dual-rail style long cluster state. The horizontal axis here is the cavity resonant frequency label ordered in a spiral permutation.

VII. Conclusions and Acknowledgements

References

[1] R. Raussendorf and H. J. Briegel, "Quantum computing via measurements only," *eprint arXiv:quant-ph/0010033*, Oct. 2000.

[2] Hans J Briegel and Robert Raussendorf, "Persistent entanglement in arrays of interacting particles," *Physical Review Letters*, vol. 86, no. 5, pp. 910, 2001.

[3] Gerald Gilbert, Michael Hamrick, and Yaakov S. Weinstein, "Efficient construction of photonic quantum-computational clusters," *Phys. Rev. A*, vol. 73, pp. 064303, Jun 2006.

[4] Philippe Jorrand and Simon Perdrix, "Unifying quantum computation with projective measurements only and one-way quantum computation," in *Moscow, Russia*. International Society for Optics and Photonics, 2005, pp. 44–51.

[5] Daniel E. Browne and Terry Rudolph, "Resource-efficient linear optical quantum computation," *Phys. Rev. Lett.*, vol. 95, pp. 010501, Jun 2005.

[6] MA Nielsen, "Universal quantum computation using only projective measurement, quantum memory, and preparation of thel 0> state," *arXiv preprint quant-ph/0108020*, 2001.

[7] R Raussendorf, J Harrington, and K Goyal, "Topological fault-tolerance in cluster state quantum computation," *New Journal of Physics*, vol. 9, no. 6, pp. 199, 2007.

[8] Daniel Gottesman and Isaac L Chuang, "Demonstrating the viability of universal quantum computation using teleportation and single-qubit operations," *Nature*, vol. 402, no. 6760, pp. 390–393, 1999.

[9] Richard Jozsa, "An introduction to measurement based quantum computation," *NATO Science Series, III: Computer and Systems Sciences. Quantum Information Processing-From Theory to Experiment*, vol. 199, pp. 137–158, 2006.

[10] R Raussendorf, J Harrington, and K Goyal, "Topological fault-tolerance in cluster state quantum computation," *New Journal of Physics*, vol. 9, no. 6, pp. 199, 2007.

[11] Chetan Nayak, Steven H. Simon, Ady Stern, Michael Freedman, and Sankar Das Sarma, "Non-abelian anyons and topological quantum computation," *Rev. Mod. Phys.*, vol. 80, pp. 1083–1159, Sep 2008.

[12] Michael A Nielsen, "Cluster-state quantum computation," *Reports on Mathematical Physics*, vol. 57, no. 1, pp. 147–161, 2006.

[13] Yaoyun Shi, "Both toffoli and controlled-not need little help to do universal quantum computation," *arXiv preprint quant-ph/0205115*, 2002.

[14] Richard Cleve and John Watrous, "Fast parallel circuits for the quantum fourier transform," in *Foundations of Computer Science, 2000. Proceedings. 41st Annual Symposium on*. IEEE, 2000, pp. 526–536.

[15] Olaf Mandel, Markus Greiner, Artur Widera, Tim Rom, Theodor W. Hänsch, and Immanuel Bloch, "Coherent transport of neutral atoms in spin-dependent optical lattice potentials," *Phys. Rev. Lett.*, vol. 91, pp. 010407, Jul 2003.

[16] W. K. Hensinger, S. Olmschenk, D. Stick, D. Hucul, M. Yeo, M. Acton, L. Deslauriers, C. Monroe, and J. Rabchuk, "T-junction ion trap array for two-dimensional ion shuttling, storage, and manipulation," *Applied Physics Letters*, vol. 88, no. 3, 2006.

[17] Guido Burkard, Daniel Loss, and David P. DiVincenzo, "Coupled quantum dots as quantum gates," *Phys. Rev. B*, vol. 59, pp. 2070–2078, Jan 1999.

[18] J. I. Cirac and P. Zoller, "Quantum computations with cold trapped ions," *Phys. Rev. Lett.*, vol. 74, pp. 4091–4094, May 1995.

[19] D. Jaksch, J. I. Cirac, P. Zoller, S. L. Rolston, R. Côté, and M. D. Lukin, "Fast quantum gates for neutral atoms," *Phys. Rev. Lett.*, vol. 85, pp. 2208–2211, Sep 2000.

[20] E. Knill, R. Laflamme, and Milburn G. J., "A scheme for efficient quantum computation with linear optics," *Nature*, vol. 409, pp. 46–52, 2000.

[21] An-Ning Zhang, Chao-Yang Lu, Xiao-Qi Zhou, Yu-Ao Chen, Zhi Zhao, Tao Yang, and Jian-Wei Pan, "Experimental construction of optical multiqubit cluster states from bell states," *Physical Review A*, vol. 73, no. 2, pp. 022330, 2006.

[22] A. I. Lvovsky, "Squeezed light," *arXiv preprint quant-ph/1401.4118*, 2001.

[23] S. Yohoyama, R. Ukai, S. C. Armstrong, C. Sornphiphatphong, T. Kaji, S. Suzuki, J. Yoshikawa, H. Yonezawa, N. C. Menicucci, and A. Furusawa, "Ultra-large-scale continuous-variable cluster states multiplexed in the time domain," *Nature Photonics*, vol. 7, pp. 982–986, 2013.

[24] Moran Chen, Nicolas C. Menicucci, and Olivier Pfister, "Experimental realization of multipartite entanglement of 60 modes of a quantum optical frequency comb," *Phys. Rev. Lett.*, vol. 112, pp. 120505, Mar 2014.